

# An Algorithm Unrolling Approach to Deep Image Deblurring

Yuelong Li<sup>†</sup>, Mohammad Tofighi<sup>†</sup>,  
Vishal Monga<sup>†</sup>, Yonina C. Eldar<sup>‡</sup>

<sup>†</sup>Pennsylvania State University    <sup>‡</sup>Technion-Israel Institute of Technology

IEEE International Conference on Acoustics, Speech and Signal Processing

May 15, 2019



# Outline

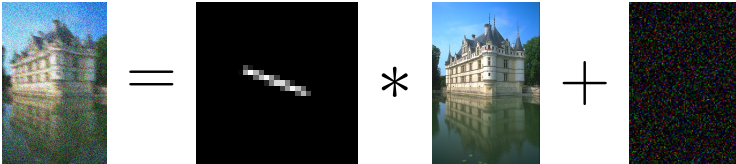
Introduction

Deblurring by Algorithm Unrolling

Experimental Results

# Background and Motivations

- ▶ Image deblurring is an essential topic in image reconstruction
  - ▶ Blurred images suffer from degraded visual quality
  - ▶ Image recognition algorithms may perform poorly when working on blurred images
- ▶ Uniform motion blur can be modeled as spatial convolutions



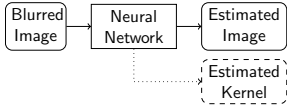
$y = k * x + n$

Blurred Image      Blur Kernel      Sharp Image      Random Noise

- ▶ Blind motion deblurring: joint estimation of  $k$  and  $x$  given  $y$ 
  - ▶ Very challenging inverse problem
  - ▶ But more practical as  $k$  is often unknown in reality

# Approaches for Recovering Deblurred Image

- ▶ Two typical categories with complementary merits

	Iterative algorithms <sup>1,2</sup>	Neural networks <sup>3,4</sup>
General idea	$\min_{\mathbf{k}, \mathbf{x}} \frac{1}{2} \ \mathbf{y} - \mathbf{k} * \mathbf{x}\ _2^2 + \lambda_1 \phi(\mathbf{x}) + \lambda_2 \psi(\mathbf{k})$	
Efficiency	Low	High
Interpretability	High	Low

- ▶ Q: is it possible to develop an approach that enjoys the merits of both worlds?

<sup>1</sup>L. Xu *et al.*, ECCV, 2010

<sup>2</sup>D. Perrone *et al.*, TPAMI, 2016

<sup>3</sup>A. Chakrabarti *et al.*, ECCV, 2016

<sup>4</sup>X. Xu, TIP, 2018

# Algorithm Unrolling

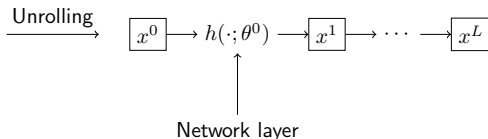
- ▶ Neural networks can be used to approximate sparse coding<sup>5</sup>
- ▶ The same idea may be used for generic iterative algorithms<sup>6,7</sup>

**Algorithm:** Input  $x^0$ , Output  $x^L$

**for**  $l = 1, 2, \dots, L$  **do**

$x^{l+1} \leftarrow h(x^l; \theta^l),$

**end for**



- ▶ For instance,  $h(\cdot)$  in <sup>5</sup> involves a soft-thresholding followed by a shrinking function.
- ▶ The unrolled network can thus be trained end-to-end
  - ▶ Optimize the algorithm parameters towards real world datasets  $\longrightarrow$  enhance performance
  - ▶ Reduce the number of required iterations  $\longrightarrow$  improve computational efficiency

---

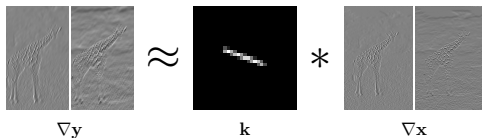
<sup>5</sup>K. Gregor *et al.*, NIPS, 2010.

<sup>6</sup>Z. Wang *et al.*, ICCV, 2015

<sup>7</sup>K. Jin *et al.*, TIP, 2017

# Generalizing Total Variation Blind Deblurring

- ▶ Deblurring can be solved in the gradient domain<sup>8</sup>
  - ▶ By enforcing gradient sparsity (total variation regularization)



- ▶ Image gradients are commonly computed by linear filtering
- ▶ Then the following optimization problem is solved:

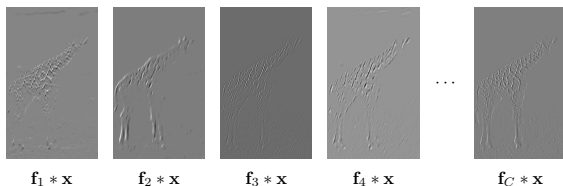
$$\begin{aligned} \min_{\mathbf{k}, \mathbf{g}_1, \mathbf{g}_2} \frac{1}{2} & \left( \|D_x \mathbf{y} - \mathbf{k} * \mathbf{g}_1\|_2^2 + \|D_y \mathbf{y} - \mathbf{k} * \mathbf{g}_2\|_2^2 \right) \\ & + \lambda_1 \|\mathbf{g}_1\|_1 + \lambda_2 \|\mathbf{g}_2\|_1 + \frac{\epsilon}{2} \|\mathbf{k}\|_2^2, \\ \text{subject to} \quad & \mathbf{1}^T \mathbf{k} = 1, \mathbf{k} \geq 0, \end{aligned}$$

- ▶ The solutions  $\mathbf{g}_1$  and  $\mathbf{g}_2$  are estimates of the gradients of the sharp image  $\mathbf{x}$ , i.e., we may expect  $\mathbf{g}_1 \approx D_x \mathbf{x}$  and  $\mathbf{g}_2 \approx D_y \mathbf{x}$

<sup>8</sup>Y. Yang *et al.*, SIAM 2008

## A Filter Domain Regularization Perspective

- ▶ Our idea: increase the number of filters to  $C > 2$  and learn their coefficients  $\{\mathbf{f}_i\}_{i=1}^C$ 
  - ▶ Use more filters to capture richer image features
  - ▶ Learn the filter coefficients by unrolling



- ▶ Formulation in the filtered domain

$$\min_{\mathbf{k}, \{\mathbf{g}_i\}_{i=1}^C} \sum_{i=1}^C \left( \frac{1}{2} \|\mathbf{f}_i * \mathbf{y} - \mathbf{k} * \mathbf{g}_i\|_2^2 + \lambda_i \|\mathbf{g}_i\|_1 \right) + \frac{\epsilon}{2} \|\mathbf{k}\|_2^2,$$

subject to  $\mathbf{1}^T \mathbf{k} = 1, \mathbf{k} \geq 0.$

# The Iterative Minimization Algorithm

- ▶ Then we cast it into the following approximation model:

$$\min_{\mathbf{k}, \{\mathbf{g}_i, \mathbf{z}_i\}_{i=1}^C} \sum_{i=1}^C \left( \frac{1}{2} \|\mathbf{f}_i * \mathbf{y} - \mathbf{k} * \mathbf{g}_i\|_2^2 + \lambda_i \|\mathbf{z}_i\|_1 + \frac{1}{2\zeta_i} \|\mathbf{g}_i - \mathbf{z}_i\|_2^2 \right) + \frac{\epsilon}{2} \|\mathbf{k}\|_2^2,$$

subject to  $\mathbf{1}^T \mathbf{k} = 1, \mathbf{k} \geq 0,$

- ▶ Minimization by half-quadratic splitting

$$\mathbf{g}_i^{l+1} \leftarrow \arg \min_{\mathbf{g}_i} \frac{1}{2} \|\mathbf{f}_i^l * \mathbf{y} - \mathbf{k}^l * \mathbf{g}_i\|_2^2 + \frac{1}{2\zeta_i^l} \|\mathbf{g}_i - \mathbf{z}_i^l\|_2^2, \quad \forall i,$$

$$\mathbf{z}_i^{l+1} \leftarrow \arg \min_{\mathbf{z}_i} \frac{1}{2\zeta_i^l} \|\mathbf{g}_i^{l+1} - \mathbf{z}_i\|_2^2 + \lambda_i^l \|\mathbf{z}_i\|_1, \quad \forall i,$$

$$\mathbf{k}^{l+1} \leftarrow \arg \min_{\mathbf{k}} \sum_{i=1}^C \frac{1}{2} \|\mathbf{f}_i^l * \mathbf{y} - \mathbf{k} * \mathbf{g}_i^{l+1}\|_2^2 + \frac{\epsilon}{2} \|\mathbf{k}\|_2^2,$$

subject to  $\mathbf{1}^T \mathbf{k} = 1, \mathbf{k} \geq 0.$

- ▶ For  $\mathbf{g}$  and  $\mathbf{z}$ , there exist close-form solutions. The problem for  $\mathbf{k}$  is also solved through series of three close-form solutions.



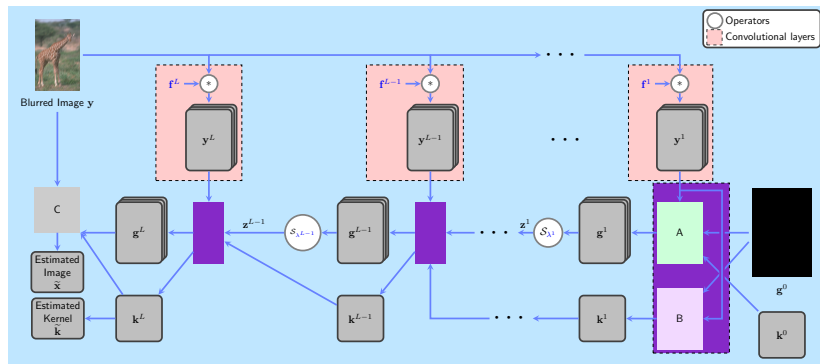
# Iterative Minimization with Dynamic Parameters

- ▶ Reconstruct image from feature maps  $\{\mathbf{g}_i\}_{i=1}^C$

$$\begin{aligned}\tilde{\mathbf{x}} &\leftarrow \arg \min_{\mathbf{x}} \frac{1}{2} \|\mathbf{y} - \mathbf{k} * \mathbf{x}\|_2^2 + \sum_{i=1}^C \frac{\eta_i}{2} \|\mathbf{f}_i * \mathbf{x} - \mathbf{g}_i\|_2^2 \\ &= \mathcal{F}^{-1} \left\{ \frac{\widehat{\mathbf{k}}^* \odot \widehat{\mathbf{y}} + \sum_{i=1}^C \eta_i \widehat{\mathbf{f}}_i^* \odot \widehat{\mathbf{g}}_i}{|\widehat{\mathbf{k}}|^2 + \sum_{i=1}^C \eta_i |\widehat{\mathbf{f}}_i|^2} \right\}\end{aligned}$$

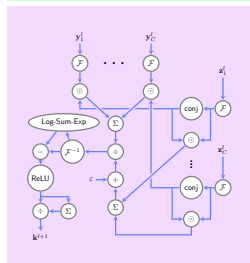
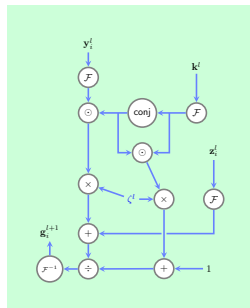
- ▶ It is beneficial to vary the parameters at different iterations
  - ▶ In particular,  $\lambda_i$ 's and  $\zeta_i$ 's may vary per iteration
- ▶ Decreasing  $\zeta_i$  ( $\zeta_i \rightarrow 0$ ) formally called continuation method
- ▶ We adopt the same strategy in network construction and use layer-specific parameters  $\{\lambda_i^l, \zeta_i^l, \mathbf{f}_i^l\}_{i,l}$

# Network Constructed through Unrolling<sup>9</sup>

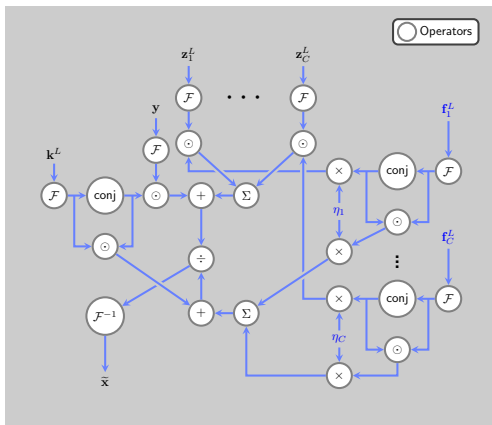


<sup>9</sup> Every learnable parameters are colored in blue

# Network Constructed through Unrolling



**A**



**C**

**B**

# Training

- ▶ Collect training image samples  $\{\mathbf{x}_t\}_{t=1}^T$  and  $\{\mathbf{k}_t\}_{t=1}^T$
- ▶ Let the  $t$ -th estimated image and kernel be  $\tilde{\mathbf{x}}_t, \tilde{\mathbf{k}}_t$
- ▶ Loss function

$$\min_{\{\mathbf{f}^l, b^l, \lambda^l\}_{l=1}^L, \eta} \sum_{t=1}^T \text{MSE} \left( \mathbf{x}_t^{\text{train}} - \tilde{\mathbf{x}}_t \left( \{\mathbf{f}^l, b^l, \lambda^l\}_{l=1}^L, \eta \right) \right) \\ + \kappa \text{MSE} \left( \mathbf{k}_t^{\text{train}} - \tilde{\mathbf{k}}_t \left( \{\mathbf{f}^l, b^l, \lambda^l\}_{l=1}^L \right) \right),$$

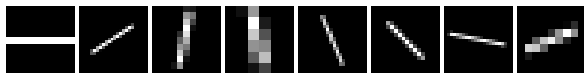
subject to  $b_i^l \geq 0, \lambda_i^l \geq 0, \quad l = 1, \dots, L, i = 1, \dots, C,$

- ▶ where  $\mathbf{f}^l = (\mathbf{f}_i^l)_{i=1}^C, b^l = (b_i^l)_{i=1}^C, \lambda^l = (\lambda_i^l)_{i=1}^C$  and  $\eta = (\eta_i)_{i=1}^C$
- ▶ Stochastic gradient descent with projection to ensure positiveness of  $b, \eta$  and  $\lambda$

# Experimental Results

## Training and Testing Setup for Linear Kernel

- ▶ Training set: 300 images from the training and validation subset of Berkeley Segmentation Data Set 500 (BSDS500)<sup>10</sup> out of 500 natural images.
- ▶ We generated 256 linear kernels by varying the length and angle of the kernels.

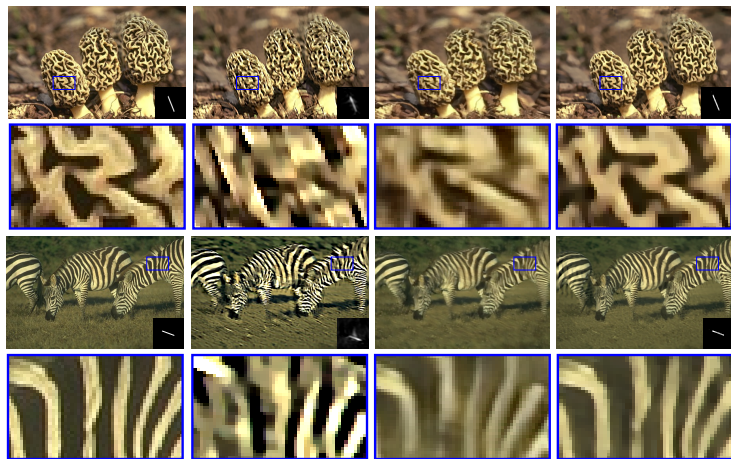


- ▶ Testing set: 200 images from the test portion of BSDS500.
- ▶ We randomly choose four kernels of different angle and length as test kernels.

---

<sup>10</sup>P. Arbelaez *et al.*, IEEE TPAMI 2011

## Visual Results on Linear Motion



(a) Groundtruth

(b) Perrone *et al.*

(c) Nah *et al.*

(d) DAU

---

Perrone *et al.*, IEEE TPAMI 2016

Nah *et al.*, CVPR 2017

# Quantitative Comparisons on Linear Motion

Table: Quantitative comparison (average of 200 images and 4 kernels).

Metrics	DAU	Perrone <i>et al.</i> <sup>13</sup>	Nah <i>et al.</i> <sup>14</sup>	Xu <i>et al.</i> <sup>15</sup>	Kupyn <i>et al.</i> <sup>16</sup>
PSNR (dB)	<b>27.30</b>	22.23	24.82	24.02	23.98
ISNR (dB)	<b>4.45</b>	2.06	1.92	1.12	1.05
SSIM	<b>0.88</b>	0.76	0.80	0.78	0.78
RMSE ( $\times 10^{-3}$ )	<b>1.67</b>	5.21	—	2.40	—

- ▶ RMSE is calculated with respect to the kernel.
- ▶ RMSE for Nah *et al.* and Kupyn *et al.*, is not reported since their methods directly recover deblurred image without estimating the kernel.

<sup>13</sup>Perrone *et al.*, IEEE TPAMI 2016

<sup>14</sup>Nah *et al.*, CVPR 2017

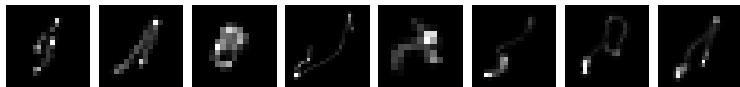
<sup>15</sup>Xu *et al.*, IEEE TIP 2018

<sup>16</sup>Kupyn *et al.*, CVPR 2018



# Training and Testing Setup for Nonlinear Kernel

- ▶ We used 330K images from the Microsoft COCO<sup>17</sup> dataset.
- ▶ We generated around 30,000 real world kernels by recording camera motion trajectories.



- ▶ Testing set: We test on *two* benchmark datasets specifically developed for evaluating blind deblurring with non-linear kernels:
  - ▶ 4 images and 8 kernels by Levin *et al.*<sup>18</sup>
  - ▶ 80 images and 8 kernels from Sun *et al.*<sup>19</sup>

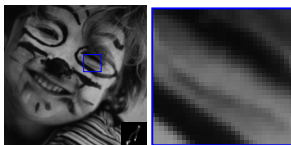
---

<sup>17</sup>T-Y. Lin *et al.*, ECCV 2014

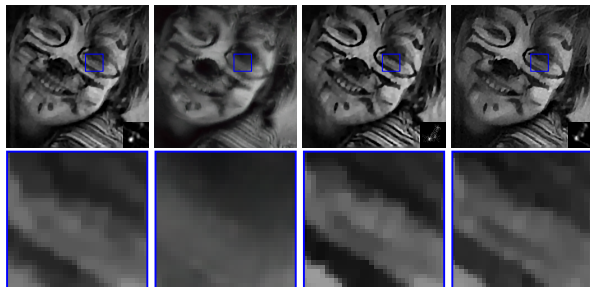
<sup>18</sup>Levin *et al.*, IEEE TPAMI, 2011

<sup>19</sup>Sun *et al.*, IEEE ICCP, 2013

# Visual Results on Non-linear Motion



(a) Groundtruth



(b) Perrone *et al.*

(c) Nah *et al.*

(d) Xu *et al.*

(e) DAU

---

Perrone *et al.*, IEEE TPAMI 2016

Nah *et al.*, CVPR 2017

Xu *et al.*, IEEE TIP 2018

## Quantitative Comparisons on Non-linear Motion

	DAU	Perrone <i>et al.</i> <sup>23</sup>	Nah <i>et al.</i> <sup>24</sup>	Xu <i>et al.</i> <sup>25</sup>
PSNR (dB)	<b>27.15</b>	26.79	24.51	26.75
ISNR (dB)	<b>3.79</b>	3.63	1.35	3.59
SSIM	<b>0.89</b>	<b>0.89</b>	0.81	<b>0.89</b>
RMSE ( $\times 10^{-3}$ )	3.87	<b>3.83</b>	—	3.98

<sup>23</sup>Perrone *et al.*, IEEE TPAMI 2016

<sup>24</sup>Nah *et al.*, CVPR 2017

<sup>25</sup>Xu *et al.*, IEEE TIP 2018

# Running Time Comparisons

	DAU	Perrone <i>et al.</i> <sup>26</sup>	Nah <i>et al.</i> <sup>27</sup>	Xu <i>et al.</i> <sup>28</sup>	Kupyn <i>et al.</i> <sup>29</sup>
Runtime (GPU/CPU) (s)	<b>0.05/1.47</b>	–/1462.90	7.32/–	2.01/6.89	0.13/10.29
Number of Parameters	<b><math>2.3 \times 10^4</math></b>	–	$2.3 \times 10^7$	$6.0 \times 10^6$	$1.2 \times 10^7$

---

<sup>26</sup>Perrone *et al.*, IEEE TPAMI 2016

<sup>27</sup>Nah *et al.*, CVPR 2017

<sup>28</sup>Xu *et al.*, IEEE TIP 2018

<sup>29</sup>Kupyn *et al.*, CVPR 2018

# Summary of Contributions

- ▶ An interpretable neural network architecture inspired by algorithm unrolling
- ▶ Superior performance, reduced number of parameters and computational benefits
- ▶ Code and datasets freely online for reproducibility<sup>30</sup>

---

<sup>30</sup>[https://scholarsphere.psu.edu/concern/generic\\_works/8sf268475m](https://scholarsphere.psu.edu/concern/generic_works/8sf268475m)

Thank you!

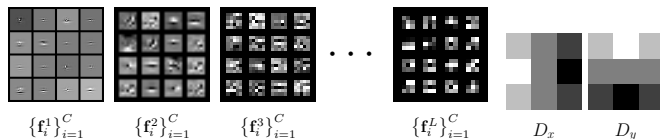
Questions?

# Cascaded Filtering

- ▶ Capture large structures first, and let details emerge later
- ▶ Correspondingly, parameterization of filter coefficients

size of  $\mathbf{f}^1 > \text{size of } \mathbf{f}^2 > \dots > \text{size of } \mathbf{f}^L$

which can be difficult to learn in practice



- ▶ Re-parametrize with small ( $3 \times 3$ ) filters  $\{\mathbf{w}_{ij}^l\}_{i,j,l}$ :

$$\mathbf{f}_i^l \leftarrow \sum_{j=1}^C \mathbf{w}_{ij}^l * \mathbf{f}_j^{l+1}.$$

# Network Flowchart

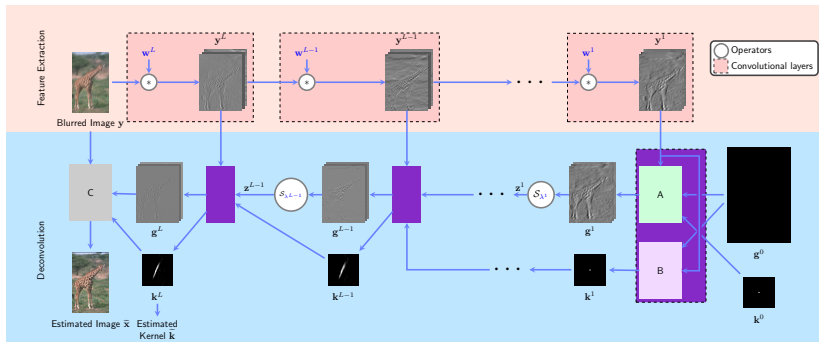


Figure: Neural network constructed through algorithm unrolling and cascaded filtering.